Fullerene/Porphyrin Multicomponent Nanostructures on Ag(110): From Supramolecular Self-Assembly to Extended Copolymers

Francesco Sedona, Marco Di Marino, Mauro Sambi,* Tommaso Carofiglio, Elisa Lubian, Maurizio Casarin, and Eugenio Tondello

Dipartimento di Scienze Chimiche, Università di Padova and Consorzio INSTM; Via Marzolo 1, 35131 Padova, Italy

ABSTRACT A novel two-step bottom-up approach to construct a 2D long-range ordered, covalently bonded fullerene/porphyrin binary nanostructure is presented: in the first place, reversible supramolecular interactions between C_{60} and 5,15-bis(4-aminophenyl)-10,20-diphenylporphyrin are exploited to obtain large domains of an ordered binary network, subsequently a reaction between fullerene molecules and the amino-groups residing on porphyrin units, triggered by thermal treatment, is used to freeze the supramolecular nanostructure with covalent bonds. The resulting nanostructure resists high temperature treatments as expected for an extended covalent network, whereas very similar fullerene/porphyrin nanostructures held together only by weak interactions are disrupted upon annealing at the same or at lower temperatures.

KEYWORDS: fullerene · porphyrins · silver · multicomponent surface self-assembly · covalent molecular networks · STM

At present, self-assembly of organic molecules on different substrates is one of the most studied approaches in order to obtain surface-supported supramolecular nanostructures with controlled dimensions and innovative properties. This bottom-up strategy can potentially become a simple, versatile, and effective approach to obtain predetermined and defect-free nanostructured two-dimensional (2D) macroscopic materials. Its success depends on our capacity to build "smart" molecular building units, able to organize themselves in a predetermined pattern by a careful exploitation of intermolecular and molecule−substrate interactions. To this end, only a detailed study of the physicochemical properties at the atomic and molecular scale of the self-organizing interfacial systems can provide the necessary know-how to build increasingly complex and chemically stable 2D functional nanosystems in a reproducible way.[1−3]

A very large number of complex two-dimensional nanonetworks has been obtained on different single crystal substrates by deposition of organic molecules whose self-assembly is driven by subtle equilibria between weak and reversible lateral (intermolecular) and vertical (molecule−substrate) interactions.[4] Specifically, dispersion and van der Waals forces,[5] dipole−dipole and donor−acceptor interactions,[6,7] hydrogen bonds,[8,9] or metal complexation[10] allow for good molecular mobility on the surface and, as a consequence, promote the formation of target structures under equilibrium conditions, which provide the apt environment for the necessary self-correction of defects, ultimately resulting in well-developed long-range order. On the other hand, these types of nanostructures are intrinsically fragile and do not resist more aggressive conditions such as high temperature thermal annealing or air exposure, they have little or no mechanical stability, and do not provide efficient intermolecular charge transport.

A nanostructure held together by strong and irreversible covalent bonds can be a solution in order to overcome these limitations.[11] Indeed, in the very past few years, different surface science groups have spent much effort in order to study the formation of covalent bonds between surface-supported organic molecules to obtain more complex molecules,[12−15] monodimensional or bidimensional ordered oligomers,[15−18] and more extended network structures.[19,20] Nevertheless, as well evidenced by Perepichka and Rosei,[21] so far the dimensions and the long-range order of these polymer nanostructures are low with respect to the arrays self-assembled through weak supramolecular interactions.

*Address correspondence to mauro.sambi@unipd.it.

Received for review May 25, 2010 and accepted August 06, 2010.

Published online August 13, 2010.
10.1021/nn101161a

© 2010 American Chemical Society

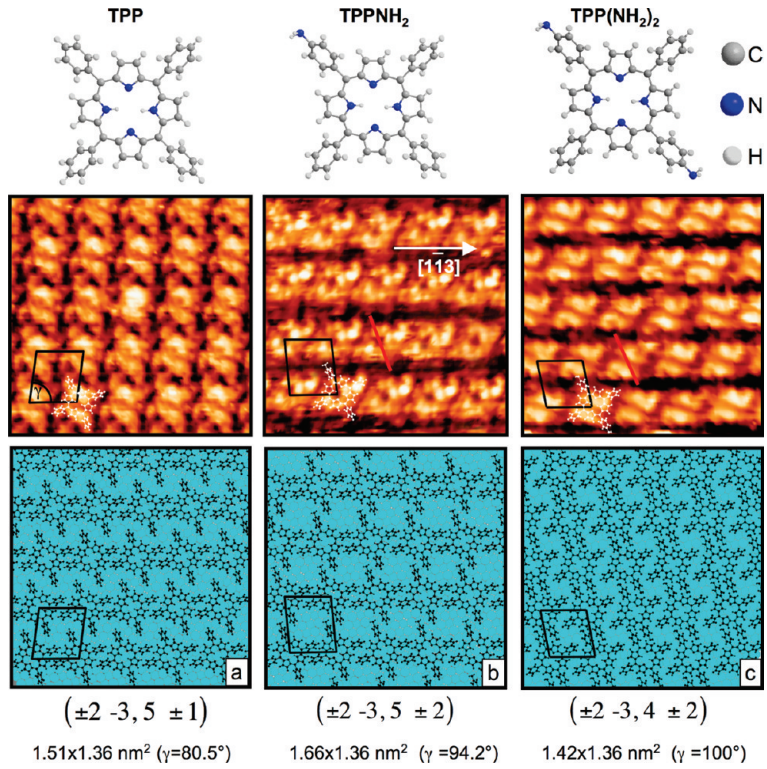

Figure 1. Single molecule models (top), high resolution STM images (center), and related superstructure models (bottom) of three different porphyrins on Ag(110): (a) TPP (7 × 7 nm^2, V = 0.53 V, I = 3.2 nA); (b) $TPPNH_2$ (7 × 7 nm^2, V = 0.03 V, I = 0.03 nA) and (c) $TPP(NH_2)_2$ (7 × 7 nm^2, V = −0.22 V, I = 2.27 nA). A molecular model (white) is superimposed to a single molecule in each STM image. The Ag(110) substrate atoms are shown as light blue circles in the bottom-most row. Unit cells are drawn in black. For every unit cell, the matrix notation with respect to the substrate and unit cell dimensions (unit vector lengths and angle γ between unit vectors) are reported. Red lines in panels b and c highlight the most probable direction of alignment of aminophenyl rings.

One of the main reasons for the high defectivity is the low activation temperature for covalent bonds formation between the molecular building units that leads to the rapid growth of large polymolecular fragments with low mobility, in turn hindering the attainment of an equilibrium ordered structure.

A possible strategy in order to obtain a large 2D long-range ordered, covalently bonded nanostructure is a two step process: one should first obtain a large 2D well-ordered supramolecular architecture exploiting weak interactions between the organic molecular modules and then stabilize this structure with covalent bonds by a thermal or phototreatment able to trigger a specific reaction between the building units which does not occur spontaneously during the self-assembly process. Within this approach, it is important that initial weak and final covalent interactions link molecules in a similar way, that is, the preorganization step should lead to a supramolecular network wherein the molecular modules are linked to each other in a such a way that the subsequent covalent bond formation implies minimal rearrangements in the superstructure, since substantial repositioning inevitably leads to a high level of disorder.[16−18]

This paper describes the advances made in our laboratory toward a bottom-up fabrication of a 2D long-range ordered, covalently bonded organic binary nanostructure composed of 5,15-bis(4-aminophenyl)-10,20-diphenylporphyrin ($TPP(NH_2)_2$ molecule in Figure 1) and C_{60} on Ag(110). This nanostructure has been obtained by means of a two-step strategy: in the first place weak, reversible interactions between C_{60} and $TPP(NH_2)_2$ are exploited to obtain very large domains of an ordered binary network. Subsequently a reaction between the amino-groups of $TPP(NH_2)_2$ and the fullerene molecules triggered by thermal treatment is used to fix the supramolecular nanostructure with covalent bonds.[22−25] All the experiments have been carried out in ultrahigh vacuum (UHV) conditions and the scanning tunneling microscopy (STM) analysis of the surface was performed at room temperature (RT). Sample bias values are reported throughout the article.

RESULTS AND DISCUSSION

As summarized in Figure 1, three types of porphyrin have been investigated: simple tetraphenylporphyrin (TPP), 5-(4-aminophenyl)-10,15,20-triphenylporphyrin ($TPPNH_2$), where one phenyl group has been substituted by a *p*-aminophenyl group, and $TPP(NH_2)_2$, where two *trans* phenyl groups have been substituted by two *p*-aminophenyl groups. In this artical the general acronym TPP collectively indicates all three tetraphenylporphyrin species when no ambiguity arises from this usage.

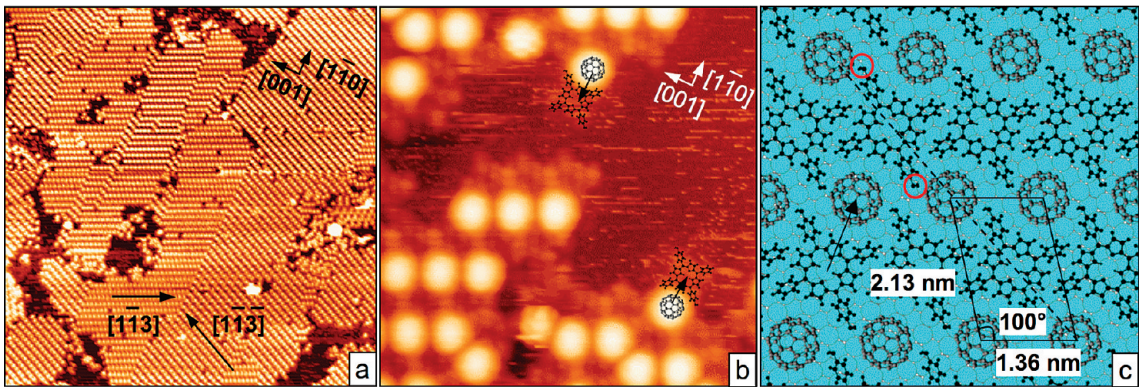

Figure 2. (±2 −3, 6 ± 3) bicomponent $TPP(NH_2)_2/C_{60}$ self-assembled nanostructure on Ag(110) obtained by annealing the system at 410 K and measured at RT. (a) Large scale STM image (140 × 140 nm², $V = -0.4$ V, $I = 4.0$ nA). (b) High resolution STM image (15 × 15 nm², $V = -0.3$ V, $I = 0.2$ nA) of a defective domain boundary: molecular models are superimposed to two $TPP(NH_2)_2/C_{60}$ couples; arrows symbolize the weak lateral intermolecular interactions between the two species aligned along the substrate [1$\bar{1}$0] direction. (c) Molecular model of the bicomponent nanostructure. The (2 −3, 6 3) superstructure unit cell is shown. Red circles highlight $-NH_2$ groups on a $TPP(NH_2)_2$ molecule.

The central and bottom rows of Figure 1 show STM images and molecular models, respectively, of TPP, $TPPNH_2$, and $TPP(NH_2)_2$ monolayer islands deposited on Ag(110) at RT. For symmetry reasons, each molecular species self-organizes in two equivalent domains rotated by 59° from each other. All overlayers form simply commensurate superstructures (integer matrix elements in matrix notation), which indicates that all molecules in each overlayer occupy equivalent adsorption sites. A tentative overlayer-substrate registry is sketched in Figure 1, bottom. From comparison of the three different unit cells, it is evident that the cell parameter aligned along the [1$\bar{1}$3] substrate direction is common to the three TPPs, whereas the second cell parameter shows different lengths and directions depending on the molecule. Therefore, on changing the number and the position of aminophenyl rings, the molecular stripe direction and the TPP-TPP nearest neighbor (NN) distance along the [1$\bar{1}$3]-oriented stripes do not change (which is reflected in the invariance of the first row in matrix notations for the three superstructures), whereas the interstripe separation is modified, giving rise to different surface densities for the three phases. This is an indication that the aminophenyl rings of $TPPNH_2$ and $TPP(NH_2)_2$ point to adjacent stripes rather than to nearest neighbor molecules within each [1$\bar{1}$3]-aligned stripe. (*i.e.,* they are aligned along the red lines in the STM images of Figure 1). Intrastripe orientation of aminophenyl rings is unlikely also for steric reasons, as already discussed in detail elsewhere.[26]

Codeposition of TPP and C_{60} submonolayers on the Ag(110) substrate held at RT has been optimized in order to obtain an approximately 1:1 ratio between the two components (as already described in ref 26) which leads to the formation of a short-range ordered bicomponent nanostructure organized in small islands.

After extensive annealing (~400 min) at 410 K, molecules self-assemble in a very large 2D long-range ordered and commensurate nanostructure, resulting from the equilibrium between weak reversible lateral TPP-C_{60} and vertical molecules−substrate interactions. Figure 2 displays STM results concerning $TPP(NH_2)_2$. The large scale STM image reported in Figure 2a shows very extended, long-range ordered and low defectivity islands (again two domains rotated by 59° from each other form for symmetry reasons), wherein single domains as large as 7000 nm² can be observed.

This complex nanostructure is strictly equivalent to the $TPPNH_2/C_{60}$ supramolecular network described in detail elsewhere.[26] This is characterized by alternating stripes of C_{60} and $TPPNH_2$ aligned along the two [1$\bar{1}$3] and [1$\bar{1}\bar{3}$] equivalent substrate directions (see Figure 2a) forming the commensurate unit cell sketched in Figure 2c, where the two species appear in a 1:1 ratio and are both in direct contact with the substrate. The $C_{60}-C_{60}$ NN distance along a stripe is 1.4 ± 0.1 nm, that is, it mirrors the intrastripe NN intermolecular distance found in the pure porphyrin phase and is substantially larger than the NN interfullerene distance (1.0 nm) in the close-packed c(4 × 4) phase produced by fullerene alone on Ag (110).[27]

The same bicomponent superstructure has been obtained by self-assembling C_{60} with all the TPPs reported in Figure 1. We conclude that the weak interactions responsible for the self-organization of this supramolecular structure are not influenced by the presence and the number of peripheral amino groups on the TPP molecules, at least in the range that has been explored. From high resolution STM images collected at the borders of ordered domains, where several isolated $C_{60}-TPP$ couples can be singled out, it is possible to infer the orientation of this weak $TPP-C_{60}$ interaction: in Figure 2b two C_{60} and two $TPP(NH_2)_2$ molecules have been evidenced with the respective molecular models in order to indicate that every $TPP(NH_2)_2$ unit "captures" a C_{60} molecule along the substrate [1$\bar{1}$0] direction (marked with black arrows) by laterally coordinating it,

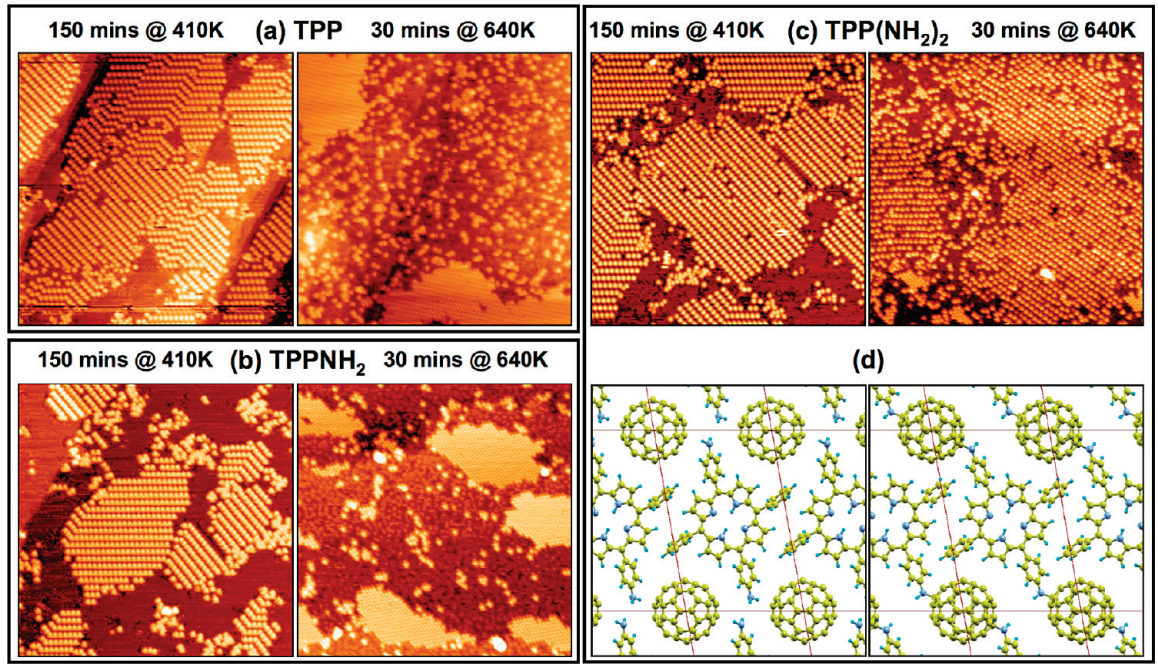

Figure 3. Different thermal stability of binary nanostructures self-assembled starting from C_{60} and (a) TPP ((left) $V = -0.8$ V, $I = 1.0$ nA; (right) $V = -0.7$ V, $I = 1.0$ nA); (b) $TPPNH_2$, ((left) $V = 0.5$ V, $I = 0.9$ nA; (right) $V = 0.8$ V, $I = 1.9$ nA), (c) $TPP(NH_2)_2$ ((left) $V = -0.5$ V, $I = 0.3$ nA; (right) $V = -0.5$ V, $I = 0.4$ nA). All STM images are 85 × 85 nm^2 in size. Annealing temperatures and times are indicated. (d) Molecular model of the supramolecular network (left) and a tentative model of the covalently linked structure (right).

possibly through a couple of adjacent peripheral phenyl rings linked to the porphyrin macrocycle. Time-lapsed STM imaging confirms the reversibility of such supramolecular interactions at the borders of the already formed bicomponent islands.

As evidenced by red circles in Figure 2c, the two aminophenyl rings of each $TPP(NH_2)_2$ molecule point toward NN C_{60} molecules rather than toward the NN $TPP(NH_2)_2$ units belonging to the same TPP stripe. Such an arrangement is required for steric reasons,[26] and it is also deduced by comparing the unit cells of the different single component porphyrin ordered phases on Ag(110) reported in Figure 1 to the unit cell of the bicomponent phase: as already remarked, the superstructure unit cell parameter along the $[1\bar{1}3]$ substrate direction is preserved (1.4 nm) on going from the single component overlayers to the bicomponent supramolecular network. In addition, the proposed orientation of aminophenyl rings is a prerequisite for the polymerization reaction discussed below.

To this point, the behavior of the three different TPP molecules with respect to C_{60} is exactly the same when the sample is annealed at 410 K. However, the thermal stability of this common superstructure is very high when $TPP(NH_2)_2$ is used as a building unit in the bicomponent self-assembly, while it is definitely lower when either TPP or $TPPNH_2$ are employed. The left columns of Figure 3 show the common nanostructure obtained using the three different porphyrins by means of a long annealing treatment (150 min) at 410 K, whereas the right column reports images of the resulting surface morphology after an additional annealing treatment of 30 min at 640 K. It appears that when one starts from TPP and $TPPNH_2$ the bicomponent ordered network is disrupted upon high temperature annealing. Phase separation occurs and consequently most C_{60} molecules segregate in close packed c(4 × 4) domains,[27] while porphyrin molecules form a disordered phase.[26,28] On the other hand, the nanostructure self-assembled starting from $TPP(NH_2)_2$ resists the thermal treatment: the local order and the dimensions of the ordered islands remain approximately unaltered. The observed high thermal stability is in line with the behavior of other covalent organic frameworks[19,20] and its high temperature limit seems to be determined by the onset of TPP degradation at about 680 K, as obtained from thermogravimetric analysis (see Supporting Information).

It is evident that the different response to the high-temperature thermal treatment strictly depends on the presence and number of amino groups on TTP molecules. The ability of amines to react with C_{60} both in self-assembled monolayers in solution[22−24] and in the solid state is well established: this property has been exploited for the production of fullerene polymers, as recently reviewed.[29] The model sketched in Figure 3d shows that the two trans amino groups on each $TPP(NH_2)_2$ molecule are very close to two C_{60} units positioned on adjacent stripes: with a few degrees of anticlockwise rotation and/or with a little shift of $TPP(NH_2)_2$ monomers, the two amino groups can be positioned at a covalent bonding distance with respect to both ad-

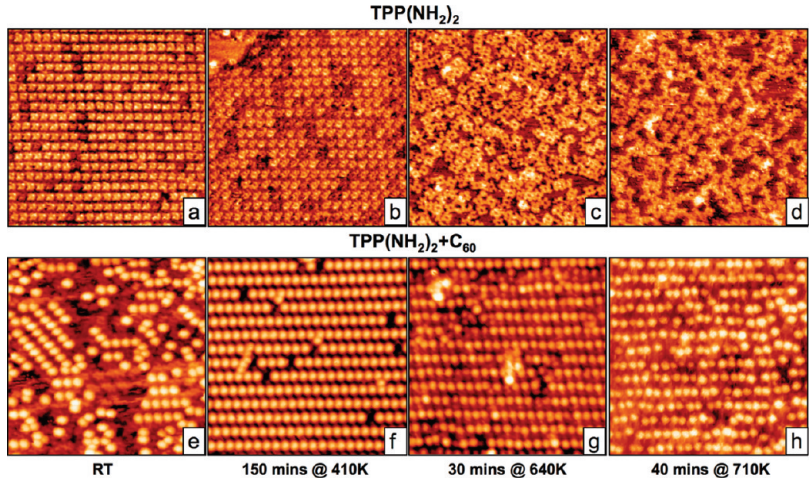

Figure 4. Thermal stability of the single component $TPP(NH_2)_2$ self-assembly (a−d, top) compared to the thermal stability of the bicomponent C_{60}−$(TPP(NH_2)_2$ system (e−h, bottom): (a) $V = -0.4$ V, $I = 3.0$ nA; (b) $V = 0.65$ V, $I = 10.0$ nA; (c) $V = -0.24$ V, $I = 3.0$ nA; (d) $V = -0.53$ V, $I = 15.0$ nA; (e) $V = -1.0$ V, $I = 1.0$ nA; (f) $V = -0.55$ V, $I = 0.35$ nA; (g) $V = 1.0$ V, $I = 2.6$ nA; (h) $V = -0.20$ V, $I = 1.6$ nA. All STM images are 15 × 15 nm^2 in size. Annealing temperatures and times are indicated for each column.

jacent C_{60} molecules, resulting in the copolymer chains sketched in Figure 3d, right, where molecules bind along the longer diagonal of the superstructure unit cell. On the basis of the available STM data, we cannot exclude the other possibility, namely the clockwise rotation of $TPP(NH_2)_2$ monomers in order to bind along the shorter diagonal of the oblique unit cell. It is worth noting that if the two bonding schemes were energetically roughly degenerate, a randomly linked 2D covalent network would occur. Quantum chemistry calculations explicitly including the interactions of both molecular species with the substrate are needed to address this interesting issue.

In summary, the peculiar high thermal stability of the binary nanostructure containing $TPP(NH_2)_2$ molecules can be explained by the fact that both amino groups on each $TPP(NH_2)_2$ unit react with nearby C_{60} molecules in the preorganized supramolecular network forming covalently bonded (-TPP-NH-$C_{60}H_2$-NH-)$_n$ copolymer chains or possibly a 2D network. Very similar water-soluble main-chain fullerene polymers with a molecular weight up to 20.0 kg/mol, wherein C_{60} units are linked through aromatic diamines, have been also reported to form in solution.[30]

To substantiate the hypothesis of covalent bonding between the molecular building units, the thermal stability of the three TPP molecules has been investigated in order to exclude that a different thermal behavior of TPP, $TPPNH_2$, and $TPP(NH_2)_2 + C_{60}$ bicomponent nanostructures is due to an intrinsically higher thermal stability of $TPP(NH_2)_2$ on Ag(110). Each TPP molecule has been deposited on Ag(110) held at RT. Three similar single component ordered phases (see the example of $TPP(NH_2)_2$, Figure 4, top) have been obtained and then annealed at 640 K for 30 min, following the same thermal treatment used for the bicomponent systems (Figure 4 (bottom) shows high resolution close ups of the $TPP(NH_2)_2 + C_{60}$ system). The resulting single component overlayer has the same characteristics, irrespective of the TPP used: the starting ordered phase is disrupted and the surface density of TPP molecules decreases by approximately 40% judging from STM images of different sample areas, while the C 1s XPS signal intensity decreases approximately 20%.

The two different numbers can be reconciled if one assumes that part of the molecules desorbs (640 K is higher than the temperature used for evaporating TPPs from the Knudsen cell) and part decomposes. In fact, desorption contributes both to STM apparent molecular surface density decrease and C 1s intensity reduction, while decomposition contributes only to the former. (Clear signs of molecular fragmentation are seen in Figure 4d, while no significant porphyrin metalation by inclusion of Ag atoms from the substrate is detected in the whole temperature range.) We conclude that the thermal stability of the three TTP molecules on Ag(110) is the same and therefore the strikingly higher stability of the $TPP(NH_2)_2/C_{60}$ bicomponent system is not related to a higher intrinsic stability of $TPP(NH_2)_2$ with respect to either TPP or $TPPNH_2$ in contact with silver. This is a further indication that the binary nanostructure containing $TPP(NH_2)_2$ is stabilized through an extended network of covalent bonds. In fact, the corresponding sequence of STM images reported in Figure 4e−h shows that no significant surface density decrease of the molecular species in the bicomponent system is observed upon heating. The notable effect of annealing between RT and 410 K is the development of large ordered domains from small supramolecular islands (Figure 4e,f). Increasing the annealing temperature to 640 K (Figure 4g) only causes a partial loss of registry of the overlayer rows with respect to the substrate, which can be attributed to small conformational adjustment of the covalently linked chains due to torsional

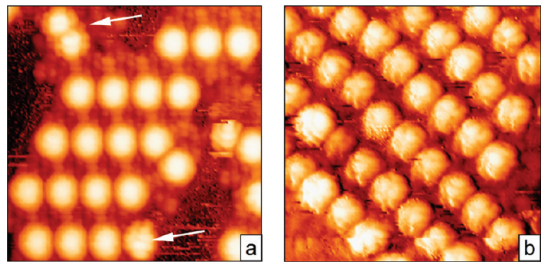

Figure 5. High resolution STM images (12 × 12 nm^2), convoluted with their respective current images, of the TPP-$(NH_2)_2/C_{60}$ bicomponent network (a) after annealing at 410 K (V = 0.3 V, I = 0.2 nA) and (b) after annealing at 640 K (V = 1.0 V, I = 0.5 nA). White arrows indicate fullerene molecules that show intramolecular fine structure at 410 K (see text).

degrees of freedom activated by the thermal treatment. The higher degree of disorder at 710 K (Figure 4h) indicates an incipient decomposition of the overlayer.

A further effect of annealing the bicomponent system at 640 K can be perceived in Figure 3c. Both left and right STM images are acquired at the same bias value. After annealing at higher temperature, C_{60} molecules in the network appear less bright than after the thermal treatment at 410 K. Quantitative measurements indeed show that upon annealing there is a ~20% decrease in apparent fullerene height with respect to the substrate in STM images at constant bias (from 5.0 ± 0.1 Å to 4.0 ± 0.6 Å at V = −0.5 V). No such effect is detected for single component C_{60} ad-islands annealed at the same temperature on the same substrate. This observation indicates a redistribution of the density of states on fullerene building units in the $TPP(NH_2)_2/C_{60}$ bicomponent network which fits the hypothesis of covalent bonding between the building units.

The latter is also supported by high resolution STM measurements where intramolecular fine structure can be detected. Figure 5 shows two high resolution STM images of the $TPP(NH_2)_2/C_{60}$ system after annealing at 410 and 640 K.

Both images are convoluted with their respective current images[31] in order to enhance the contrast of intramolecular fine structure features. While no such features are detected on the majority of fullerenes in the supramolecular network after annealing at 410 K, they are clearly seen after annealing at 640 K on all fullerene units, which indicates that C_{60} molecules maintain substantial rotational or at least librational degrees of freedom in the supramolecular network (which is typical for predominantly ionic C_{60}−substrate interactions,[32] at least as far as C_{60} does not form close-packed islands which can stabilize a specific orientation with respect to the surface), while such degrees of freedom are frozen after high temperature annealing, again in accordance with the proposed covalent network formation. It is worth noting that after annealing at 410 K (Figure 5a) a few molecules do show intermolecular fine structure, as indicated by white arrows. The frozen conformation of the two "defective" C_{60} molecules in the upper left corner can be attributed to their direct mutual interaction (they are at a distance of approximately 1.0 nm from each other, that is, at the van der Waals NN distance in close packed single component fullerene ad-islands).[27] The molecule highlighted in the bottom part of the image belongs to the regular bicomponent network. However, it differs from its siblings for its definite orientation, giving rise to the observed intramolecular fine structure in the STM appearance. These observations indicate (a) that the C_{60}−$TPP(NH_2)_2$ lateral interactions in the supramolecular network are weaker and less directionally specific than the C_{60}−C_{60} direct van der Waals interactions in fullerene clusters and close-packed C_{60} ad-islands and (b) that at 410 K only a tiny minority of fullerene molecules reacts with $TPP(NH_2)_2$ even after extended annealing times, thus setting a lower temperature limit for the occurrence of the covalent bonds formation.

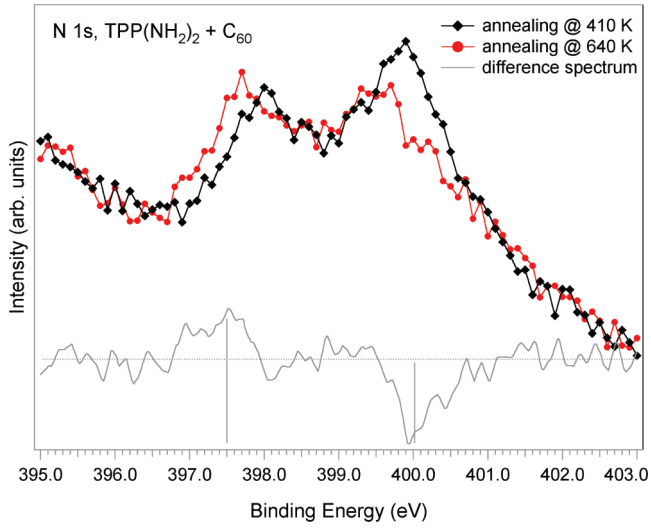

Figure 6. Al Kα-excited N 1s XP spectrum of the $TPP(NH_2)_2/C_{60}$ bicomponent network after annealing at 410 K (black squares) and at 640 K (red circles). Both spectra are referenced to the Ag $3d_{5/2}$ photoemission peak, whose BE (368.2 eV) does not change upon annealing. The difference spectrum is also shown.

In-situ spectroscopic evidence for the occurrence of the polymerization reaction at 640 K is also provided by X-ray photoelectron spectroscopy (XPS). The N 1s region shows characteristic changes in the course of the reaction, which are in agreement with the proposed bonding scheme.

Figure 6 shows the N 1s XP spectrum of $TPP(NH_2)_2$ molecules belonging to the $TPP(NH_2)_2/C_{60}$ bicomponent network on Ag(110) after annealing at the two relevant temperatures. The spectrum after the thermal treatment at 410 K consists of two components at 400.1 and 398.2 eV, which are assigned to pyrrolic (−NH−) and iminic (−N=) nitrogen, respectively, in accordance with previous studies.[33−36] In pristine TPP (spectrum not shown) the two components have the same intensity, reflecting the equal number of nitrogen atoms of the two types in the molecule.

In $TPP(NH_2)_2$ the high BE component is more intense, since the contribution of the two primary amino

groups (at BE = 400.0 eV)[24] cannot be resolved from the pyrrolic contribution. After annealing at 640 K, the high BE component decreases, while a new component appears at 397.5 eV, whose intensity roughly equals the intensity decrease around 400.0 eV (see the difference spectrum in Figure 6). Almost the same binding energy shift is observed in the literature when surface-grafted primary alkylamines react with C_{60} to form R−NH−C_{60}H adducts.[24] We conclude that the XPS spectra of the N 1s region provide a fingerprint for the occurrence of the polymerization reaction.

The obtained covalently linked network is particularly robust and is resistant to air and water exposure (see Supporting Information).

To better understand the occurrence of the fullerene−aminoporphyrin reaction, equimolar amounts of $TPPNH_2$ and C_{60} have been mechanically blended with a pestle in an agate mortar. The solid mixture was then heated for 1 h at 85 °C. TLC analysis (petroleum ether/ethyl acetate 3:2 v/v) showed the complete disappearance of the porphyrin (R_f = 0.56) and the formation of a new product (R_f = 0.79). Both UV−vis and ^{13}C NMR analysis (see Supporting Information) confirmed that this new product contained the spectroscopic signatures of the porphyrin and the fullerene units and were different from those obtained for a 1:1 mixture of the two compounds. This result shows that the addition reaction between $TPPNH_2$ and C_{60} takes place smoothly even at low temperatures. As shown here, a substantially higher temperature is required to trigger the reaction in the surface-supported supramolecular aggregate, which is a key for the successful two-step synthesis of the covalently linked nanostructure. A higher reaction temperature on the surface with respect to solution and solid state may be traced back to a substantially reduced entropic term due to frozen orientational degrees of freedom in the supramolecular network, possibly coupled to an active role of the substrate in the form of charge transfer from Ag to C_{60},[37,38] which is expected to partially hinder the nucleophilic attack of the amino-groups to fullerene.

In conclusion, we have shown that an extended, ordered, and covalently linked bicomponent molecular superstructure can be obtained by thermal triggering of covalent bonds formation in a preorganized supramolecular network of C_{60} and $TPP(NH_2)_2$. These results show promising potential for the synthesis of highly ordered networks of surface-supported functional copolymers. In particular, they point to a possible route for the simple and effective one-pot synthesis of extended regular networks of covalently bonded donor−acceptor (D−A) arrays for efficient charge-separation through the choice of properly functionalized D and A building units. The possibility to extend the polymer conjugation into the second dimension[21] is currently also investigated through the choice of the fully aminated $TPP(NH_2)_4$ molecule as a precursor for the bicomponent molecular self-assembly.

METHODS

Synthesis of $TPP(NH_2)_2$. 5,15-bis(4-aminophenyl)-10,20-diphenylporphyrin was prepared as previously described by Vincente *et al.*[39] by nitration of $TPPH_2$ (purchased from EGA-CHEMIE, Germany) with sodium nitrite in TFA followed by reduction with $SnCl_2$/HCl. Purification was carried out by column chromatography (Al_2O_3, CH_2Cl_2/petroleum ether 8:2 v/v eluent).

Reaction between $TPPNH_2$ and C_{60}. A solid mixture of 5-(4-aminophenyl)-10,15,20-triphenylporphyrin and C_{60} in 1:1 molar ratio was heated at 85 °C. After 1 h, TLC analysis (silica gel, eluent petroleum ether/ethyl acetate 3:2 v/v) confirmed the complete disappearance of $TPPNH_2$ and the formation of a new product containing both the features of porphyrin and C_{60}, as confirmed by ^{13}C NMR and UV−vis spectroscopy (see Supporting Information).

Sample Preparation in UHV. The Ag(110) crystal was cleaned by repeated cycles of 1 keV Ar^+ sputtering and annealing at 820 K until a clean surface with sufficiently large terraces was confirmed by STM imaging. The three different TPP molecules were deposited from a PBN crucible held at temperatures between 500 and 590 K, whereas C_{60} (99% purity) was sublimed at temperatures between 850 and 890 K from a tungsten crucible. The Ag specimen was kept at room temperature during sublimations. Both crucibles were outgassed for a long time to avoid impurities during the depositions onto the substrate.

Scanning Tunneling Microscopy (STM). The experiments were performed with an Omicron scanning tunneling microscope (VT-STM) operating in UHV at a base pressure of 2×10^{-10} mbar. The STM measurements were carried out at RT in constant current mode, using a Pt−Ir tip. The sample bias voltage (V) and the tunneling current (I) are indicated for all STM images. STM images were analyzed with the WSxM software.[40]

X-ray Photoelectron Spectroscopy (XPS). Measurements were performed *in situ* at RT by means of a Scienta M-780 Al Kα (1486.6 eV) monochromatic X-ray source and a Scienta SES-100 photoelectron analyzer fitted to the STM preparation chamber. The overall instrumental resolution measured at the Fermi edge of the clean Ag sample was 0.3 eV. The binding energies are referenced to the Fermi edge (BE ≡ 0).

Acknowledgment. D. Forrer and A. Vittadini are gratefully acknowledged for useful discussions. This work has been partially funded by MIUR (PRIN 2008, Project n. 2008MXZEAS: "Molecular SPACE") and by the University of Padova (Progetto Strategico HELIOS and Progetti di Ricerca di Ateneo - CPDA088228/08).

Supporting Information Available: Spectroscopic (^{13}C NMR and UV−vis) characterization of the solid state reaction between $TPPNH_2$ and C_{60}; thermogravimetric analysis of TPP, $TPPNH_2$ and $TPP(NH_2)_2$; STM image of air- and water-exposed sample. This material is available free of charge *via* the Internet at http://pubs.acs.org.

REFERENCES AND NOTES

1. Whitesides, G. M.; Grzybowski, B. Self-Assembly at All Scales. *Science* **2002**, *295*, 2418.
2. Barth, J. V.; Costantini, G.; Kern, K. Engineering Atomic and Molecular Nanostructures at Surfaces. *Nature* **2005**, *437*, 671–679.
3. Elemans, J. A. A. W.; Lei, S.; De Feyter, S. Molecular and Supramolecular Networks on Surfaces: from Two-Dimensional Crystal Engineering to Reactivity. *Angew. Chem., Int. Ed.* **2009**, *48*, 7298–7332.
4. Theobald, J. A.; Oxtoby, N. S.; Phillips, M. A.; Champness, N. R.; Beton, P. H. Controlling Molecular Deposition and Layer Structure with Supramolecular Surface Assemblies. *Nature* **2003**, *424*, 1029–1031.
5. Casarin, M.; Di Marino, M.; Forrer, D.; Sambi, M.; Sedona, F.; Tondello, E.; Vittadini, A.; Barone, V.; Pavone, M.

Coverage-Dependent Architectures of Iron Phthalocyanine on Ag(110): A Comprehensive STM/DFT Study. *J. Phys. Chem. C* **2010**, *114*, 2144–2153.
6. Bonifazi, D.; Kiebele, A.; Stöhr, M.; Cheng, F.; Jung, T.; Diederich, F.; Spillmann, H. Supramolecular Nanostructuring of Silver Surfaces *via* Self-Assembly of Fullerene and Porphyrin Modules. *Adv. Funct. Mater.* **2007**, *17*, 1051–1062.
7. Yoshimoto, S.; Honda, Y.; Ito, O.; Itaya, K. Supramolecular Pattern of Fullerene on 2D Bimolecular "Chessboard" Consisting of Bottom-Up Assembly of Porphyrin and Phthalocyanine Molecules. *J. Am. Chem. Soc.* **2008**, *130*, 1085–1092.
8. Huang, Y. L.; Chen, W.; Li, H.; Ma, J.; Pflaum, J.; Wee, A. T. S. Tunable Two-Dimensional Binary Molecular Networks. *Small* **2010**, *6*, 70–75.
9. Blunt, M. O.; Russell, J. C.; del Carmen Giménez-Lopez, M.; Garrahan, J. P.; Lin, X.; Schröder, M.; Champness, N. L.; Beton, P. H. Random Tiling and Topological Defects in a Two-Dimensional Molecular Network. *Science* **2008**, *322*, 1077–1081.
10. Dmitriev, A.; Spillmann, H.; Lin, N.; Barth, J. V.; Kern, K. Modular Assembly of Two-Dimensional Metal−Organic Coordination Networks at a Metal Surface. *Angew. Chem., Int. Ed.* **2003**, *42*, 2670–2673.
11. Gourdon, A. On-Surface Covalent Coupling in Ultrahigh Vacuum. *Angew. Chem., Int. Ed.* **2008**, *47*, 6950–6953.
12. Weigelt, S.; Schnadt, J.; Tuxen, A. K.; Masini, F.; Bombis, C.; Busse, C.; Isvoranu, C.; Ataman, E.; Lægsgaard, E.; Besenbacher, F.; Linderoth, T. R. Formation of Trioctylamine from Octylamine on Au(111). *J. Am. Chem. Soc.* **2008**, *130*, 5388–5389.
13. Weigelt, S.; Busse, C.; Bombis, C.; Knudsen, M. M.; Gothelf, K. V.; Strunskus, T.; Will, C.; Dahlboom, M.; Hammer, B.; Laegsgaard, E.; Besenbacher, F.; Linderoth, T. R. Covalent Interlinking of an Aldehyde and an Amine on a Au(111) Surface in Ultrahigh Vacuum. *Angew. Chem., Int. Ed.* **2007**, *46*, 9227–9230.
14. Weigelt, S.; Bombis, C.; Busse, C.; Knudsen, M. K.; Gothelf, K. V.; Laegsgaard, E.; Besenbacher, F.; Linderoth, T. R. Molecular Self-Assembly from Building Blocks Synthesized on a Surface in Ultrahigh Vacuum: Kinetic Control and Topo-Chemical Reactions. *ACS Nano* **2008**, *2*, 651–660.
15. Jensen, S.; Früchtl, H.; Baddeley, C. J. Coupling of Triamines with Diisocyanates on Au(111) Leads to the Formation of Polyurea Networks. *J. Am. Chem. Soc.* **2009**, *131*, 16706–16713.
16. Matena, M.; Riehm, T.; Stöhr, M.; Jung, T. A.; Gade, L. H. Transforming Surface Coordination Polymers into Covalent Surface Polymers: Linked Polycondensed Aromatics through Oligomerization of *N*-Heterocyclic Carbene Intermediates. *Angew. Chem., Int. Ed.* **2008**, *47*, 2414–2417.
17. In't Veld, M.; Iavicoli, P.; Haq, S.; Amabilino, D. B.; Raval, R. Unique Intermolecular Reaction of Simple Porphyrins at a Metal Surface Gives Covalent Nanostructure. *Chem. Commun.* **2008**, 1536–1538.
18. Grill, L.; Dyer, M.; Lafferentz, L.; Persson, M.; Peters, M. V.; Hecht, S. Nano-architectures by Covalent Assembly of Molecular Building Blocks. *Nat. Nanotechnol.* **2007**, *2*, 687–691.
19. Zwaneveld, N. A. A.; Pawlak, R.; Abel, M.; Catalin, D.; Gigmes, D.; Bertin, D.; Porte, L. Organized Formation of 2D Extended Covalent Organic Frameworks at Surfaces. *J. Am. Chem. Soc.* **2008**, *130*, 6678–6679.
20. Bieri, M.; Treier, M.; Cai, J.; Aït-Mansour, K.; Ruffieux, P.; Gröning, O.; Gröning, P.; Kastler, M.; Rieger, R.; Feng, X.; Müllen, K.; Fasel, R. Porous Graphenes: Two-Dimensional Polymer Synthesis with Atomic Precision. *Chem. Commun.* **2009**, 6919–6921.
21. Perepichka, D. F.; Rosei, F. Extending Polymer Conjugation into the Second Dimension. *Science* **2009**, *323*, 216–217.
22. Backer, S. A.; Suez, I.; Fresco, Z. M.; Rolandi, M.; Fréchet, J. M. J. Covalent Formation of Nanoscale Fullerene and Dendrimer Patterns. *Langmuir* **2007**, *23*, 2297–2299.
23. Chen, K.; Caldwell, W. B.; Mirkin, C. A. Fullerene Self-Assembly onto $(MeO)_3(CH_2)_3NH_2$-Modified Oxide Surfaces. *J. Am. Chem. Soc.* **1993**, *115*, 1193–1194.
24. Zhang, X; Teplyakov, A. V. Adsorption of C_{60} Buckminster Fullerenes on an 11-Amino-1-undecene-Covered Si(111) Substrate. *Langmuir* **2008**, *24*, 810–820.
25. Sapurina, I.; Mokeev, M.; Lavrentev, V.; Zgonnik, V.; Trchová, M.; Hlavatá, D.; Stejskal, J. Polyaniline Complex with Fullerene C_{60}. *Eur. Polym. J.* **2000**, *36*, 2321–2326.
26. Di Marino, M.; Sedona, F.; Sambi, M.; Carofiglio, T.; Lubian, E.; Casarin, M.; Tondello, E. STM Investigation of Temperature-Dependent Two-Dimensional Supramolecular Architectures of C_{60} and Amino-tetraphenylporphyrin on Ag(110). *Langmuir* **2010**, *26*, 2466–2472.
27. David, T.; Gimzewski, J. K.; Purdie, D.; Reihl, B.; Schlitter, R. Epitaxial Growth of C_{60} on Ag(110) Studied by Scanning Tunneling Microscopy and Tunneling Spectroscopy. *Phys. Rev. B* **1994**, *50*, 5810–5813.
28. More precisely, the thermal stability of the nanostructure self-assembled starting either from TPP or $TPPNH_2$ is even lower: after annealing for several tens of minutes at 470 K, a new porous superstructure appears,[26] which is characterized by a 3:1 C_{60}:TPP ratio. If the temperature of the thermal treatment is increased to 520 K the c(4 × 4) C_{60} single component islands phase-separate, as reported in Figure 3.
29. Giacalone, F.; Martin, N. Fullerene Polymers: Synthesis and Properties. *Chem. Rev.* **2006**, *106*, 5136–5190.
30. Samal, S.; Choi, B.-J.; Geckeler, K. E. The First Water-Soluble Main-Chain Polyfullerene. *Chem. Commun.* **2000**, 1373–1374.
31. Casarin, M.; Forrer, D; Orzali, T.; Petukhov, M.; Sambi, M.; Tondello, E.; Vittadini, A. Strong Bonding of Single C_{60} Molecules to (1 × 2)-Pt(110): an STM/DFT Investigation. *J. Phys. Chem. C* **2007**, *111*, 9365–9373.
32. Wang, L. T.; Cheng, H. P. Rotation, Translation, Charge Transfer, and Electronic Structure of C_{60} on Cu(111) Surface. *Phys. Rev. B* **2004**, *69*, 045404.
33. Gottfried, J. M.; Flechtner, K.; Kretschmann, A.; Lukasczyk, T.; Steinrück, H.-P. Direct Synthesis of a Metalloporphyrin Complex on a Surface. *J. Am. Chem. Soc.* **2006**, *128*, 5644–5645.
34. Flechtner, K.; Kretschmann, A.; Bradshaw, L. R.; Walz, M.-M.; Steinrück, H.-P.; Gottfried, J. M. Surface-Confined Two-Step Synthesis of the Complex (Ammine)(Meso-tetraphenylporphyrinato)−Zinc(II) on Ag(111). *J. Phys. Chem. C* **2007**, *111*, 5821–5824.
35. Shubina, T. E.; Marbach, H.; Flechtner, K.; Kretschmann, A.; Jux, N.; Buchner, F.; Steinrück, H.-P.; Clark, T.; Gottfried, J. M. Principle and Mechanism of Direct Porphyrin Metalation: Joint Experimental and Theoretical Investigation. *J. Am. Chem. Soc.* **2007**, *129*, 9476–9483.
36. Buchner, F.; Flechtner, K.; Bai, Y.; Zillner, E.; Kellner, I.; Steinrück, H.-P.; Marbach, H.; Gottfried, J. M. Coordination of Iron Atoms by Tetraphenylporphyrin Monolayers and Multilayers on Ag(111) and Formation of Iron−Tetraphenylporphyrin. *J. Phys. Chem. C* **2008**, *112*, 15458–15465.
37. Magnano, E.; Vandré, S.; Cepek, C.; Goldoni, A.; Laine, A. D.; Currò, G. M.; Santaniello, A.; Sancrotti, M. Substrate−Adlayer Interaction at the C_{60}/Ag(110) Interface, Studied by High Resolution Synchrotron Radiation. *Surf. Sci.* **1997**, *377*−*379*, 1066–1070.
38. Goldoni, A.; Cepek, C.; Magnano, E.; Laine, A. D.; Vandré, S.; Sancrotti, M. Temperature Dependence of the Electronic Structure Near E_F and Electron−Phonon Interaction in C_{60}/Ag(100) Single Layers. *Phys. Rev. B* **1998**, *58*, 2228–2232.
39. Luguya, R.; Jaquinod, L.; Fronczek, F. R.; Vicente, M. G. H.; Smith, K. M. Synthesis and Reactions of Meso-(*p*-Nitrophenyl)porphyrins. *Tetrahedron* **2004**, *60*, 2757–2763.
40. Horcas, I.; Fernandez, R.; Gomez-Rodriguez, J. M.; Colchero, J.; Gomez-Herrero, J.; Baro, A. M. WSxM: A Software for Scanning Probe Microscopy and a Tool for Nanotechnology. *Rev. Sci. Instrum.* **2007**, *78*, 013705.